



Published in final edited form as:

*Nat Microbiol.* ; 2: 17007. doi:10.1038/nmicrobiol.2017.7.

## A *Wolbachia* Deubiquitylating Enzyme Induces Cytoplasmic Incompatibility

John F. Beckmann<sup>1,†</sup>, Judith A. Ronau<sup>1,†</sup>, and Mark Hochstrasser<sup>1,2,\*</sup>

<sup>1</sup>Department of Molecular Biophysics & Biochemistry, Yale University, 266 Whitney Avenue, New Haven, CT 06520. USA

<sup>2</sup>Department of Molecular, Cellular, & Developmental Biology, Yale University, 266 Whitney Avenue, New Haven, CT 06520. USA

*Wolbachia* are obligate intracellular bacteria<sup>1</sup> that infect arthropods, including ~two-thirds of insect species.<sup>2</sup> *Wolbachia* manipulate insect reproduction by enhancing their inheritance through the female germline. The most common alteration is cytoplasmic incompatibility (CI),<sup>3–5</sup> wherein eggs from uninfected females fail to develop when fertilized by sperm from *Wolbachia*-infected males. By contrast, if female and male partners are both infected, embryos are viable. CI is a gene-drive mechanism impacting population structure<sup>6</sup> and causing reproductive isolation,<sup>7</sup> but its molecular mechanism remained unknown. We show that a *Wolbachia* deubiquitylating enzyme (DUB) induces CI. The CI-inducing DUB, CidB, cleaves ubiquitin from substrates and is encoded in a two-gene operon; the other protein, CidA, binds CidB. Binding is strongest between cognate partners in *cidA-cidB* homologs. In transgenic *Drosophila*, the *cidA-cidB* operon mimics CI when sperm introduce it into eggs; a catalytically inactive DUB does not induce sterility. Toxicity is recapitulated in yeast by CidB alone; this requires DUB activity but is rescued by coexpressed CidA. A paralogous operon involves a putative nuclease (CinB) rather than a DUB; analogous binding, toxicity and rescue in yeast were observed. These results identify a CI mechanism involving interacting proteins secreted into germline cells by *Wolbachia* and suggest new methods for insect control.

The mechanism of CI is frequently modeled as a modification-rescue (or toxin-antidote) system in which sperm undergo a *Wolbachia*-mediated modification event<sup>8,9</sup> that can be conditionally rescued in the egg by a *Wolbachia*-encoded factor (Fig. 1a, b).<sup>10–12</sup> Normally,

Users may view, print, copy, and download text and data-mine the content in such documents, for the purposes of academic research, subject always to the full Conditions of use:[http://www.nature.com/authors/editorial\\_policies/license.html#terms](http://www.nature.com/authors/editorial_policies/license.html#terms)

\*corresponding author (mark.hochstrasser@yale.edu).

†Equal contribution

### Data Availability

The data that support the findings of this study are available from the corresponding author upon request.

### Author Contributions

John F. Beckmann and Judith A. Ronau are equal contributors in conception and performance of the experiments as well as writing of the manuscript.

Mark Hochstrasser conceived experiments and wrote the manuscript.

All yeast and fly strains and all DNA reagents described here will be made available upon publication. We have no competing interests to declare.

upon fertilization the sperm-derived pronucleus undergoes nuclear envelope breakdown and exchanges protamines for maternal histones. Subsequently, male and female pronuclei juxtapose (but do not fuse) and undergo DNA replication prior to the first zygotic mitosis. Chromosomes from both pronuclei synchronously condense, align at metaphase, and separate in anaphase.<sup>13</sup> In CI crosses, paternal chromatin fails to condense properly for the first cell cycle. This induces lethal missegregation and bridging of paternal DNA at anaphase.<sup>14,15</sup> This specific cytological phenotype at the first zygotic mitosis is a central hallmark of CI, distinguishing it from other types of post-zygotic male sterility.

Although *Wolbachia* infect both male and female germlines, the bacteria are removed in the later stages of spermatid differentiation. In a previous proteomic study, we had therefore searched for *Wolbachia* (*wPip* strain) proteins associated with *Wolbachia*-modified mosquito sperm and identified the protein WPA0282.<sup>16</sup> The *wPa\_0282* gene is part of a two-gene operon (Fig. 1c). Given our identification (see below) of the second gene product, WPA0283, as a CI-inducing DUB (deubiquitylating enzyme), we have renamed the genes *cidA* (*wPa\_0282*) and *cidB* (*wPa\_0283*). Ubiquitin is a small polypeptide that posttranslationally modifies many proteins and has numerous functions. Protein ubiquitylation is highly dynamic and is reversed by cellular DUBs.<sup>17</sup> Genetic evidence from diverse *Wolbachia* strains suggests that the modification and rescue functionalities of CI arise from at least two independent genes, similar to bacterial toxin-antidote systems.<sup>10</sup> Most such toxin-antidote systems studied have simple two-gene operon structures. Therefore, we hypothesized that the *cidA-cidB* operon products might be the executors of CI.

As *Wolbachia* strains evolve within different host species, they accumulate mutations in their corresponding CI systems and become bidirectionally incompatible.<sup>3</sup> This could potentially be due to their respective CI-regulating factors having evolved mutually exclusive binding specificities.<sup>10</sup> Interestingly, *Wolbachia* genomes from *Culex pipiens* mosquitoes show extensive genetic duplication and divergence of the putative CI-inducing operons, possibly accounting for multiple incompatibilities. The *Wolbachia* strain *wPip*, for example, has two related operons (Fig. 1c, d). The second operon encodes proteins related to CidA and CidB, but the downstream gene encodes what is likely to be a functional PD-(D/E)XK nuclease domain (DUF1703)<sup>18</sup> rather than a DUB (Fig. 1d); we have provisionally named the two genes in this operon as *cinA* (*wPa\_0294*) and *cinB* (*wPa\_0295*). CidB and CinB may share a common nuclease ancestor (Supplementary Figure. 1; Fig. 1c, dotted lines), but the predicted nuclease active-site residues are not maintained in CidB. Importantly, the predicted functional status of the enzymatic components of these operons correlates with ability of diverse *Wolbachia* strains to induce bi-directional CI (see Supplemental Discussion).

In bacterial toxin-antidote systems, the two components bind one another. We therefore expressed recombinant tagged constructs of the *cidA-cidB* operon proteins (Supplementary Figures 2, 3) and examined their interactions. Pull-down of His6-tagged CidA from extracts of *E. coli* expressing both His6-CidA and CidB also brought down the CidB protein (Supplementary Figure 3a, b). We observed similar binding of the cognate partners His6-CinA and CinB (Supplementary Figure 3c, d).

Differential binding affinities of operon-encoded partners might account for the bidirectional incompatibilities noted above. This model would predict that proteins derived from the same operon associate in preference to their noncognate partners<sup>19</sup> from other operons. To test this, we purified His6-tagged copies of CidB and CinB. These proteins were incubated with extracts of the corresponding FLAG-tagged CidA and CinA proteins, and binding was assessed (Fig. 1f). Indeed, binding was much stronger between cognate proteins from the same operon. These results are consistent with a model in which operon-specific differences in partner binding affinities underlie the bidirectional incompatibilities and partial rescues seen in genetic crosses with different *Wolbachia* strains.

When divergent CI-causing *Wolbachia* strains are introduced into different insect species by microinjection, CI is recapitulated.<sup>20,21</sup> This indicates that *Wolbachia* CI factors can operate in a broad range of hosts (Supplemental Discussion). To test the modification-rescue model for CI in a heterologous eukaryotic host, we expressed the Cid and Cin proteins in the yeast *Saccharomyces cerevisiae* (Fig. 2). Both CidB and CinB (but not CidA or CinA) caused temperature-sensitive growth inhibition when expressed in yeast. Growth was rescued by coexpression of the cognate partners, CidA and CinA, respectively. When the predicted cysteine protease active site in CidB<sup>22</sup> was mutated from Cys to Ala (CidB\* in Fig. 2a), temperature-sensitive lethality was lost. Similarly, upon mutation of the three predicted nuclease active-site residues in CinB (CinB\*, Fig. 2a), temperature-sensitive lethality was again no longer observed. Changes in protein levels of the modifiers cannot account for the loss of toxicity, at least in the case of CidB\* (Supplementary Figure 4). Importantly, only the correctly matched cognate partners rescued growth when coexpressed with CidB or CinB (Fig. 2b). Toxicity and rescue for both operons was seen in two different yeast backgrounds (BY4741 and W303a). These results with yeast show that the cognate *Wolbachia* operon-encoded factors display toxicity and rescue, respectively; that toxicity depends on the (putative) enzymatic activities (see below) of the CidB and CinB proteins; and finally, that suppression of toxicity *in vivo* correlates with cognate protein binding preferences *in vitro*.

Next we sought to characterize the enzymatic activity of CidB. We initially expected it would behave like a protease specific for the small ubiquitin-like modifier (SUMO) protein since it bears a C48/Ulp1-like domain;<sup>22</sup> however, the purified protein did not cleave fluorogenic SUMO-AMC or SUMO-peptide fusions. By contrast, CidB reacted with a ubiquitin-based suicide inhibitor, HA-ubiquitin vinyl methyl ester (HA-UbVME); its reactivity was similar to that of a well-characterized DUB, UCH37 from *Trichinella spiralis*<sup>23</sup> (Fig. 3a, Supplementary Figure 5d). Enzyme activity was tested against polyubiquitin chains with isopeptide linkages (C-terminal ubiquitin carboxyl group linked to a ubiquitin lysine  $\epsilon$ -amino group) involving either Lys48 or Ly63 residues or against ubiquitin dimers linked through each of the seven different ubiquitin lysines. CidB could hydrolyze all seven lysine-linked isopeptide bonds, but had a preference for Lys63 linkages in quantitative assays (Fig. 3b, c; Fig. Supplementary Figure 5, Supplemental Discussion). The enzyme did not cleave Met1-linked (linear) diubiquitin even after overnight incubation. Finally, both CidB and CidB<sup>wMel</sup> hydrolyzed Ub-AMC, and to a much lesser extent, the ubiquitin-like substrate Nedd8-AMC (Supplementary Figure 6). A CidB-C1025A catalytic mutant (CidB\*) was inactive against Ub-AMC. Despite the ability to cleave multiple substrates *in vitro*, CidB appears to have a restricted substrate range in cells, as bulk

ubiquitin conjugates in yeast were not detectably altered by CidB expression (Supplementary Figure 5c).

Because CidA binds CidB and suppresses CidB toxicity in yeast, we tested whether CidA inhibited CidB DUB activity *in vitro*. A 100-fold molar excess of CidA failed to inhibit CidB modification by UbVME, cleavage of Ub chains (Fig. 3a, b, last lane of each panel), or Ub-AMC hydrolysis. Therefore, CidA likely rescues toxicity in yeast by some other means, such as control of its localization. This would have the advantage that the related CidA and CinA proteins could interact in similar ways to enzymatically distinct cognate factors, such as those with DUB and nuclease domains.

To test the ability of the *cidA-cidB* operon to induce CI in an insect in the absence of *Wolbachia* infection, we cloned expression constructs into the germline-optimized pUASp-attB vector<sup>24</sup> for transgenic insertion into *D. melanogaster* by the site-directed  $\Phi$ C31 integrase<sup>25</sup> (Supplementary Figure 7). The multiple independent transgenic flies each had a fusion of the *cidA-cidB* ORFs linked by a T2A viral peptide sequence that causes ribosomal skipping such that CidA and CidB are produced as separate proteins<sup>26</sup> (Supplementary Figure b). After transgenesis, we verified attB/P recombination by PCR, confirmed that our fly lines were not infected by native *Wolbachia* strains, and verified transgene expression by reverse-transcription PCR (Supplementary Figure 7c–e). Strikingly, males expressing the transgenic operon displayed a fully penetrant sterility in matings with wild-type females (four biological replicates with two independent attP insertion sites; Fig. 4a; Supplementary Figure 7). By contrast, females transgenic for the *cidA-cidB* operon were fertile, indicating that the operon caused embryonic lethality only if it was inherited from males. Mutational inactivation of the CidB DUB (CidB-C1025A) in transgenic inserts eliminated the ability of the insert to cause male sterility (Fig. 4a, “operon\*”).

Attempts to rescue the CI-like phenotype with transgenic females expressing either CidA alone or the full operon were not successful. This precludes the unequivocal assignment of the “rescue” component of CI to the *cidA-cidB* operon. Potential reasons for these negative results are provided in the Supplemental Discussion.

Previous reports have implicated genes in CI pathways without quantitative cytological analysis of the first mitotic cell cycle. Others have identified host genes which can induce CI-like sterility<sup>27</sup>, but a *Wolbachia* gene that can precisely mimic CI cytology at the first embryonic mitosis has never been identified. To verify that *cidA-cidB* specifically induced CI rather than an alternative type of sterility, we determined whether embryos from crosses with *cidA-cidB* transgenic males recapitulated CI-defining cytological and embryonic defects (Fig. 4b). These defects include impaired male pronuclear chromatin condensation at metaphase and delayed chromosome separation and bridging at anaphase. All were observed in the transgenic crosses. Of the embryos analyzed during the first post-fertilization mitosis, 88% showed these CI-like defects compared to only 3% in WT crosses (Fig. 4c). Of the transgenic embryos that were left to develop for 24 hours, 60% arrested prior to blastoderm formation (“early,” Fig. 4d). Of the 20% of embryos that developed to segmentation, 69% showed segmentation deformities<sup>28</sup> (Supplementary Figure 8a, b). These specific developmental defects recapitulate those of CI embryos.<sup>13–15,28,29</sup> Thus, the defects

produced by *cidA-cidB* expression in males replicate the established developmental abnormalities in CI-inducing crosses from *Wolbachia*-infected males.

Research on CI was pioneered over 60 years ago using intraspecific crosses of the mosquito *C. pipiens*.<sup>3</sup> The *Wolbachia*-CI link was made in 1971,<sup>4</sup> but the molecular mechanism has remained obscure. Our data provide strong evidence that the *Wolbachia cidA-cidB* operon is responsible for CI. The most parsimonious interpretation of our yeast and transgenic fly data is an adaptation of the modification-rescue framework first proposed by Hurst<sup>12</sup> and Werren<sup>30</sup> in which CidB is the modifier and CidA would function as the rescue factor. *Wolbachia* bacteria have a type IV secretion system that could translocate the CidA and CidB proteins into the host cytoplasm. The *cidA-cidB* is encoded within a WO prophage (see Suppl. Discussion), so virus-induced cell lysis would be another potential route of transmission. In analogy to many toxin-antidote systems in free-living bacteria, we propose that within the fertilized egg of an incompatible cross, CidA is rapidly inactivated or degraded. Unless CidA is supplied by a maternal *Wolbachia* infection in the egg's cytoplasm, the paternally supplied CidB enzyme would become active. CidA alone might also not be sufficient for rescue in the egg; additional *Wolbachia* or host factors might be required, possibly for co-localization of the cognate partners. The exact targets of the CidB DUB enzyme (and putative CinB nuclease) and the detailed molecular pathway of *cidA-cidB*-induced CI also remain to be determined.

Regardless of these outstanding mechanistic questions, our results suggest immediate potential practical benefits. The complete sterility induced by *cidA-cidB* in male insects and the lack of obvious harmful effects on their fitness suggest that release of such transgenic sterile males could be highly effective for population control of many insect pests or human disease vectors. An obvious application would be in limiting mosquito vectors responsible for transmission of dengue and Zika viruses or malarial parasites.

## Materials and Methods

### DNA manipulation

DNA was purified from *Wolbachia*-infected insects according to Beckmann and Fallon.<sup>31</sup> Genes from *cid* and *cin* operons were cloned from DNA of *wPip*-infected *C. pipiens* Buckeye mosquitoes<sup>16</sup> and from YW *wMel*-infected *D. melanogaster* flies. PCR products were amplified with primers listed in Supplemental Table 1 using PhusionHF DNA polymerase (New England Biolabs), gel-purified, and ligated into various plasmid vectors, including the pBAD (ThermoFisher; arabinose induction), pET (ThermoFisher; IPTG induction), pCold-GST (gift from Chittaranjan Das; IPTG induction) and pGEX (GE Healthcare; IPTG induction) *E. coli* expression vectors. All plasmid inserts were fully sequenced at the Yale Keck Foundation DNA sequencing facility. Point mutations were introduced by QuikChange mutagenesis (Stratagene). Further modifications such as truncations or tag additions were carried out using SLIM.<sup>32</sup>

## Protein purification for pull-down analysis of His6-tagged proteins

The procedure followed was a slight modification of the Dynabeads manufacturer's protocol (Novex). Recombinant proteins were initially expressed in the *E. coli* TOP10F' strain, but since they were prone to proteolytic cleavage by Lon protease (Supplementary Figure 2), we switched to expression in BL21-AI (ThermoFisher) or Rosetta DE3 (Novagen) *E. coli* strains, which lack Lon. Large (2 L) or small (100 ml) cultures were grown in Luria Broth (LB) at 37°C with vigorous shaking to 0.5 OD at  $\lambda_{600\text{ nm}}$  and induced with either 0.02% arabinose (pBAD) or 1 mM IPTG (pET). Protein induction in most cases was allowed to proceed overnight at 18°C. Cell pellets were resuspended in wash buffer (50 mM sodium phosphate [pH 8.0]; 300 mM NaCl; 0.01% Tween-20; 5 mM  $\beta$ -mercaptoethanol; 10 mM imidazole) and lysed by either sonication or French press. Lysates were incubated for 10–60 min at 4°C with HisPur cobalt resin or Ni-NTA agarose resin (both Qiagen).

For His6-tagged protein pull-down assays, bead-bound tagged proteins were incubated with bacterial extracts containing target proteins for 1 h at 4°C. The resin was washed, and bound proteins were eluted at 4°C with 1 bead volume of elution buffer containing 300 mM imidazole. For large-scale purifications of His6-tagged proteins, eluates isolated by the same method were concentrated to ~0.3 ml in a 10 kDa-cutoff concentrator (Amicon). Protein concentrations were determined either by densitometry on a Syngene G:box with GeneTools software using BSA as a standard or by Bradford assay (Bio-Rad).

## Purification of proteins for kinetic assays

To obtain purified enzymes for kinetic analysis of DUB activity, CidB (residues 762–1143) and CidB<sup>wMel</sup> (797–1128) were overproduced as glutathione-S-transferase (GST) fusions in *E. coli* with minor modifications to the protocol described previously.<sup>33</sup> Briefly, large-scale cultures were grown to late exponential phase in LB and were induced with 0.3 mM IPTG. Following induction at 37°C for 4 h, cells were harvested and lysed via French press. Proteins were purified by GST-affinity chromatography using glutathione-agarose (Thermo Scientific). After removal of the GST tag with PreScission protease (GE Biosciences), the protein was further purified by size-exclusion chromatography using a HiLoad Superdex S75 PG column (GE Biosciences) in a buffer consisting of 50 mM Tris-HCl (pH 7.6), 150 mM NaCl, and 1 mM DTT. All protein samples were concentrated, aliquoted, flash frozen, and stored at –80°C until use. Prior to use, concentrations were carefully determined both spectrophotometrically at 280 nm and by BCA Assay (Thermo Scientific).

Lys63-linked and Lys48-linked ubiquitin dimers were synthesized enzymatically using Lys63Arg, Lys48Arg, and Asp77 (mouse) ubiquitin mutants according to a previously described method.<sup>33,34</sup> Enzymes required for formation of Lys63 diubiquitin were human E1 (pGEX6P1 vector), Uev1a (pGEX6P1), Ubc13 (pGEX6P1), Lys63Arg ubiquitin (pET26b), and Asp77 ubiquitin (pET26b). These were purified separately and mixed in a reaction buffer containing 80 mM Tris-HCl (pH 7.6), 20 mM ATP, 20 mM MgCl<sub>2</sub>, and 1 mM DTT. Synthesis of Lys48 diubiquitin used a reaction consisting of human E1, CDC34 (pET16b), Lys48Arg ubiquitin (pET26b) and Asp77 ubiquitin. All reactions proceeded overnight at room temperature and were quenched by addition of a 10-fold excess of Buffer A [50 mM NaOAc (pH 4.5)]. Unreacted ubiquitin and enzymes utilized for the reaction were separated



from newly formed diubiquitin using MonoS cation-exchange chromatography (GE Biosciences). Lys63- and Lys48-linked ubiquitin dimers were eluted using a linear gradient of Buffer A mixed with Buffer B [50 mM NaOAc (pH 4.5), 1 M NaCl], and then buffer exchanged to 50 mM Tris-HCl (pH 7.6), 150 mM NaCl, 1 mM DTT. All diubiquitin samples were concentrated, aliquoted, flash frozen, and stored at  $-80^{\circ}\text{C}$  until use.

### SDS-polyacrylamide gel electrophoresis and Western immunoblotting

Standard SDS-PAGE gel analysis was carried out in a range of gel concentrations. Proteins were either stained with GelCode Blue (ThermoFisher) or transferred to PVDF Immobilon-P transfer membranes (0.45  $\mu\text{M}$  pore size) (Sigma-Aldrich) for immunoblot analysis.<sup>35</sup> Antibodies utilized for immunoblotting were: mouse anti-tetraHis (Qiagen, 1:4,000); mouse anti-FLAG M2 (Sigma, 1:10,000); rabbit anti-ubiquitin (Dako, 1:1000); mouse 16B12 anti-HA (Covance, 1:1000); and mouse anti-PGK (yeast phosphoglycerate kinase) (Molecular Probes, 1:20,000). Secondary antibodies used were: sheep anti-mouse NA931V (GE Healthcare, 1:10,000) and donkey anti-rabbit NA934V (GE Healthcare, 1:5,000). Membranes used for anti-His blotting required blocking of nonspecific binding with 3% (w/v) BSA and extensive washing. Other immunoblot analyses used 5% milk for blocking.

### Diubiquitin cleavage assays

Cleavage assays were carried out using CidB(762–1143) following a previously published protocol.<sup>33</sup> Briefly, 250 nM CidB was incubated in a reaction buffer of 50 mM Tris (pH 7.6), 20 mM KCl, 5 mM  $\text{MgCl}_2$ , and 1 mM DTT with Lys63-linked diubiquitin concentrations ranging from 20–120  $\mu\text{M}$ . In assays using Lys48-linked diubiquitin, 400 nM CidB was used. All reactions were carried out at room temperature for 10 min (Lys63 reactions) or 15 min (Lys48 reactions) and were quenched by the addition of 5x SDS-PAGE sample buffer. Ubiquitin standards ranging from 6–40  $\mu\text{M}$  were used to generate a standard curve, enabling quantification of ubiquitin produced from each diubiquitin cleavage reaction using ImageJ software.<sup>36</sup> To account for the release of two ubiquitin moieties (P and P') from a single reaction, the initial rates of each reaction were divided by 2. All kinetic data were analyzed with Kaleidagraph Version 4.1.3b1 and could be fit to the Michaelis-Menten equation:  $V_i = (V_{\text{max}}[S])/(K_M + [S])$  where [S] is the concentration of substrate. We also tested reactivity of full length CidB with all seven potential ubiquitin lysine linkages by incubating 1  $\mu\text{M}$  enzyme with 1  $\mu\text{M}$  diubiquitin for 1 h, 4h or overnight at  $37^{\circ}\text{C}$  using the Ub<sub>2</sub> Explorer Panel (LifeSensors). Lastly, we incubated 50 nM CidB with 500 nM mixtures of Lys63-linked or Lys48-linked polyubiquitin chains (ranging in size from 2–7 ubiquitins; Boston Biochem) for 20 min to 4 h at  $37^{\circ}\text{C}$ . Error bars are standard deviations.

### Ubiquitin-AMC and UBL-AMC hydrolysis assays

Ubiquitin (Ub) and ubiquitin-like protein (UBL) with C-terminal 7-amido-4-methylcoumarin adducts (Ub-AMC and UBL-AMC) were used for hydrolysis assays as described previously.<sup>23</sup> Briefly, a CidB fragment encompassing the DUB domain (residues 762–1143) was diluted to a final concentration of 5 nM in reaction buffer (50 mM Tris, pH 7.6, 0.5 mM EDTA, 0.1% bovine serum albumin, 5 mM DTT). Prior to addition of the Ub or UBL-linked AMC substrate (Ub-AMC, Nedd8-AMC, SUMO1/2-AMC, and ISG15-AMC; Boston Biochem), the enzyme was pre-incubated at  $30^{\circ}\text{C}$  for 5 min, and all reactions

proceeded at 30°C. Apart from the ISG15-AMC substrate (excitation/emission 380 nm/460 nm), hydrolysis of the Ub/UBL-AMC substrates as a function of time was monitored via excitation/emission at 345 nm/445 nm using a SynergyMix plate reader (BioTek, Winooski, VT). A standard curve using AMC (Sigma Aldrich) concentrations ranging from 0–50 nM was prepared in reaction buffer to allow quantification of the amount of hydrolyzed substrate. Despite testing human ISG15-AMC and SUMO1/2-AMC with several concentrations of CidB (up to 400 nM), we failed to detect any AMC release. Substrate concentrations ranging from 50 nM to 2 μM were mixed with 5 nM and 25 nM CidB in Ub-AMC and Nedd8-AMC assays, respectively. Initial velocities were extrapolated from the linear portion of the curve and plotted as a function of substrate concentration. As the catalytic activity exhibited a linear response to substrate over the concentration range tested, data could not be fit to the Michaelis-Menten equation. Data were instead fit to the equation  $v/[E] = k_{cat}/K_M[S]$ , where [E] and [S] are the concentrations of enzyme and substrate, respectively. All enzymatic assays were carried out in triplicate and analyzed using Kaleidagraph Version 4.1.3b1. Error bars are standard deviations.

### Generation of a covalent CidB-UbVME adduct

To test for formation of a covalent complex between CidB and the suicide DUB inhibitor UbVME, 1 μM CidB was mixed with 1 μM HA-UbVME (a gift from Michael Sheedlo and Chittaranjan Das, Purdue University). After adjusting the pH to 8, reactions were carried out for 30 min at room temperature and quenched by mixing with 5x SDS sample buffer, and the products were run on a gradient SDS-PAGE gel. Following electrotransfer to a PVDF filter, the filter was incubated, as outlined above, with anti-HA antibodies, followed by secondary antibody. To probe the effect of CidA on formation of a covalent complex between CidB and UbVME, 100-fold excess CidA was incubated with CidB at room temperature for 40 min prior to the addition of UbVME. Complex formation with full-length CidB did not elicit a visible mobility shift on the gel. To demonstrate complex formation via mobility shift, we purified a smaller construct, comprising only the DUB domain (CidB<sup>844–1096</sup>) and reacted it with UbVME (Supplemental Figure 5d).

### Yeast methods

Analysis of yeast growth that is displayed in figures utilized the BY4741 strain background. Rescue experiments were replicated in the W303a background. DNA fragments used for expression in yeast were subcloned from *E. coli* vectors by restriction digest or PCR amplification and ligated into yeast vectors (Supplemental Table 1). The 2-micron plasmids pYES2 (*URA3*) and p425GAL (*LEU2*) both had the *GAL1* promoter and *CYCI* terminator and were utilized for galactose-induced expression of *Wolbachia* genes in yeast.<sup>37</sup> Expression from the low-copy CEN vector pRS416GAL1 was also utilized. For serial dilutions of yeast cells, cultures were grown overnight in non-inducing minimal synthetic media lacking either uracil, leucine, or both depending on the plasmid(s) used for expression. Cells were pelleted by centrifugation, washed with sterile water, and spotted in 5-fold serial dilution from an initial 0.05 OD<sub>600</sub> concentration on solid minimal SD media containing either 2% galactose or glucose and lacking either uracil, leucine, or both. Plates were placed at 30, 32, 34, and 37°C for 3 d.



## Drosophila genetic analysis

An initial *cidA-T2A-cidB* operon construct was synthesized and codon optimized for *Drosophila* by Genscript and cloned into the pUC57 vector (Supplementary Figure 7b). Genes were then subcloned from the mother construct into the pUASp-attB vector<sup>24,38</sup> by PCR and restriction digest. The full-length operon construct pUASp-attB-*cidA-T2A-cidB* was unstable in TOP10F' bacterial cells and prone to degradation. The plasmid was stabilized in CopyCutter EPI400 cells (Epicentre). All constructs for transgenesis in the pUASp-attB vector were fully sequenced and verified to lack spurious mutations.

DNA constructs were sent to BestGene Inc. for microinjection of *D. melanogaster* embryos. Fly backgrounds #9744 and #9750 (containing different attP insertion sites on the 3<sup>rd</sup> chromosome) were chosen for site-directed attP/B integration by the  $\Phi$ C31 integrase. Red-eyed flies were selected and screened by BestGene. Upon receipt of transgenic lines, we independently verified attP/B integration by PCR using primers 509 and 510 (#9744; 0.5kb product) or 509 and 511 (#9750; 0.7 kb product; Supplemental Table 1), which amplified a product only if site-specific recombination had occurred. We also verified that our #9744, #9750, and <sup>w</sup>CS (WT) strains were uninfected with native *Wolbachia* isolates that might interfere with crossing data. This was done using PCR to amplify the *cidA*<sup>wMeI</sup> gene. As a positive DNA control, we amplified a ~200 bp product of *D. melanogaster rps3*. The basal P-element promoter in pUASp-attB induced sufficient expression to induce phenotypes without a Gal4 driver. This was confirmed by reverse transcription-PCR (RT-PCR) analysis carried out by purifying RNA with TRIzol reagent (Ambion) according to the manufacturer's specifications from pools of 20 male flies. RNA was further purified with by RNeasy (Qiagen) and treated with DNase I. Complementary DNA was synthesized using the iScript cDNA Synthesis Kit (BioRad), and the cDNA was used as template for PCR reactions with primers that amplified either *cidB* or *rps3*.

Flies were maintained at room temperature on a standard diet. For CI analysis, two males (<3 d old) were mated to 10 virgin females in an individual tube. 1 tube of 12 flies was one N. Adult flies were removed after 10 days of egg laying, and fecundity was assessed by counting eclosed adult progeny. In the case of the crosses that led to sterility, flies were allowed to lay eggs until they died in the tube; they never produced offspring. To assess the cytology of early embryos resulting from an incompatible cross with *cidA-cidB* transgenic males, ~300 virgin female <sup>w</sup>CS flies were placed in a collection container with ~100 transgenic *cidA-cidB* males and put on apple juice plates with yeast paste for 2 d. Embryos were then collected by a brush and sieve every 15 min, dechorionated in 50% bleach, and fixed immediately in a solution of 5 ml heptane, 2 ml 2.5x PBS, 500  $\mu$ l 0.5 M EDTA, and 1 ml of 37% fresh formaldehyde.<sup>39</sup> The fixing solution (10 ml) was kept in a clear glass scintillation vial to allow visualization of liquid phase layers and eggs. Vitelline membranes were removed by replacing the heptane top layer with 2 volumes of methanol and vigorous shaking. Sunken de-vitellinated embryos were collected with a Pasteur pipette, washed three times with methanol, and stored overnight at 4°C before they were rehydrated with PBTA<sup>39</sup> and stained with Hoechst 33342 dye (ThermoFisher Scientific) at 1:1000 in PBTA. Stained embryos were washed and mounted on glass slides and sealed under a cover slip with nail

polish. Microscopic analysis of the embryos was performed on a Zeiss Axioskop microscope using a 100X/ 1.4 NA objective lens.

Variations in the cytological quantifications are shown as the standard deviation of the mean of triplicate samples of 200 embryos (Fig. 4d). Polar bodies were used as a landmark. Images where polar bodies were not observed were excluded from the data in Fig. 4c. Images were captured by AxioVision Re.4.8 software and adjusted for contrast and assembled in Photoshop (Adobe). The images confirmed that the *cidA-cidB* transgenic males, while sterile, mated and successfully fertilized eggs. In cases where nuclei were not well visualized in a single plane of focus, a Z-stack maximum projection was created in ImageJ.

Crosses aimed at testing rescue of *cidA-cidB*-induced lethality were performed by first creating various heterozygous [*GAL4; UAS-cidA*] flies. These were generated by crossing [*yw; UAS-cidA*] homozygous virgin females with male driver strains that are expected to express Gal4 during oogenesis: #4442: *nanos*-Gal4, #32551: *ubiquitin*-Gal4, #44241: *oskar*-Gal4, #7062: *MATa*-Gal4 (all transgenes on the 2<sup>nd</sup> chromosome), or #31777: *MTD*-Gal4, which has multiple *GAL4* inserts on all three large chromosomes including *nanos*-Gal4, *nanos*-Gal4:VP16, and *otu*-Gal4. These double heterozygotes were then mated with *cidA-cidB* males to test fecundity. Fly stocks were obtained from the Bloomington Stock Center or were gifts.

## Supplementary Material

Refer to Web version on PubMed Central for supplementary material.

## Acknowledgments

We thank Ann Fallon, Robert Tomko Jr., and Adela Chavez for critical review of the manuscript; Lisa Klasson for sharing preliminary data; Horacio Frydman and Lynn Cooley for fly lines; John Carlson, Karen Menuz, Paul Graham, and Cain Yam for support with fly experimentation; Christian Schlieker for use of instruments; and Chittaranjan Das and Michael Sheedlo for HA-Ub-VME. Funding was provided by USDA-NIFA postdoctoral fellowship 2014-67012-22268 (JFB), the Marion Brooks-Wallace fellowship (JFB), and NIH grant GM053756 (MH).

## References

- Hertig M, Wolbach SB. Studies on Rickettsia-like micro-organisms in insects. J Med Res. 1924; 44:329-U322. [PubMed: 19972605]
- Werren JH, Baldo L, Clark ME. Wolbachia: master manipulators of invertebrate biology. Nat Rev Microbiol. 2008; 6:741–751. [PubMed: 18794912]
- Laven, H. Chapter 7: Speciation and Evolution in *Culex pipiens*. Elsevier; 1967. p. 251
- Yen JH, Barr AR. New hypothesis of the cause of cytoplasmic incompatibility in *Culex pipiens* L. Nature. 1971; 232:657–658. [PubMed: 4937405]
- Hunter MS, Perlman SJ, Kelly SE. A bacterial symbiont in the Bacteroidetes induces cytoplasmic incompatibility in the parasitoid wasp *Encarsia pergandiella*. Proc Biol Sci. 2003; 270:2185–2190. [PubMed: 14561283]
- Turelli M, Hoffmann AA. Rapid spread of an inherited incompatibility factor in California *Drosophila*. Nature. 1991; 353:440–442. [PubMed: 1896086]
- Bordenstein SR, O'Hara FP, Werren JH. Wolbachia-induced incompatibility precedes other hybrid incompatibilities in *Nasonia*. Nature. 2001; 409:707–710. [PubMed: 11217858]

8. Clark ME, Veneti Z, Bourtzis K, Karr TL. Wolbachia distribution and cytoplasmic incompatibility during sperm development: the cyst as the basic cellular unit of CI expression. *Mech Dev.* 2003; 120:185–198. [PubMed: 12559491]
9. Presgraves DC. A genetic test of the mechanism of Wolbachia-induced cytoplasmic incompatibility in *Drosophila*. *Genetics.* 2000; 154:771–776. [PubMed: 10655228]
10. Poinot D, Charlat S, Mercot H. On the mechanism of Wolbachia-induced cytoplasmic incompatibility: confronting the models with the facts. *BioEssays : news and reviews in molecular, cellular and developmental biology.* 2003; 25:259–265.
11. Bourtzis, K., Braig, HR., Karr, TL. Chapter 14 Cytoplasmic Incompatibility. Vol. 1. CRC Press; 2003.
12. Hurst LD. The Evolution of Cytoplasmic Incompatibility or When Spite Can Be Successful. *J Theor Biol.* 1991; 148:269–277. [PubMed: 2016892]
13. Tram U, Ferree PM, Sullivan W. Identification of Wolbachia--host interacting factors through cytological analysis. *Microbes and infection / Institut Pasteur.* 2003; 5:999–1011.
14. Callaini G, Dallai R, Riparbelli MG. Wolbachia-induced delay of paternal chromatin condensation does not prevent maternal chromosomes from entering anaphase in incompatible crosses of *Drosophila simulans*. *Journal of cell science.* 1997; 110(Pt 2):271–280. [PubMed: 9044057]
15. Reed KM, Werren JH. Induction of paternal genome loss by the paternal-sex-ratio chromosome and cytoplasmic incompatibility bacteria (Wolbachia): a comparative study of early embryonic events. *Molecular reproduction and development.* 1995; 40:408–418. [PubMed: 7598906]
16. Beckmann JF, Fallon AM. Detection of the Wolbachia protein WPIP0282 in mosquito spermathecae: implications for cytoplasmic incompatibility. *Insect biochemistry and molecular biology.* 2013; 43:867–878. [PubMed: 23856508]
17. Ronau JA, Beckmann JF, Hochstrasser M. Substrate specificity of the ubiquitin and Ubl proteases. *Cell research.* 2016
18. Knizewski L, Kinch LN, Grishin NV, Rychlewski L, Ginalski K. Realm of PD-(D/E)XK nuclease superfamily revisited: detection of novel families with modified transitive meta profile searches. *BMC structural biology.* 2007; 7:40. [PubMed: 17584917]
19. Mercot H, Charlat S. Wolbachia infections in *Drosophila melanogaster* and *D. simulans*: polymorphism and levels of cytoplasmic incompatibility. *Genetica.* 2004; 120:51–59. [PubMed: 15088646]
20. Bian G, et al. Wolbachia invades *Anopheles stephensi* populations and induces refractoriness to *Plasmodium* infection. *Science.* 2013; 340:748–751. [PubMed: 23661760]
21. Xi Z, Khoo CC, Dobson SL. Wolbachia establishment and invasion in an *Aedes aegypti* laboratory population. *Science.* 2005; 310:326–328. [PubMed: 16224027]
22. Li SJ, Hochstrasser M. A new protease required for cell-cycle progression in yeast. *Nature.* 1999; 398:246–251. [PubMed: 10094048]
23. Morrow ME, et al. Stabilization of an unusual salt bridge in ubiquitin by the extra C-terminal domain of the proteasome-associated deubiquitinase UCH37 as a mechanism of its exo specificity. *Biochemistry.* 2013; 52:3564–3578. [PubMed: 23617878]
24. Rorth P. Gal4 in the *Drosophila* female germline. *Mech Dev.* 1998; 78:113–118. [PubMed: 9858703]
25. Groth AC, Fish M, Nusse R, Calos MP. Construction of transgenic *Drosophila* by using the site-specific integrase from phage phiC31. *Genetics.* 2004; 166:1775–1782. [PubMed: 15126397]
26. Diao F, White BH. A novel approach for directing transgene expression in *Drosophila*: T2A-Gal4 in-frame fusion. *Genetics.* 2012; 190:1139–1144. [PubMed: 22209908]
27. Clark ME, Heath BD, Anderson CL, Karr TL. Induced paternal effects mimic cytoplasmic incompatibility in *Drosophila*. *Genetics.* 2006; 173:727–734. [PubMed: 16489228]
28. Callaini G, Riparbelli MG, Giordano R, Dallai R. Mitotic defects associated with cytoplasmic incompatibility in *Drosophila simulans*. *J Invertebr Pathol.* 1996; 67:55–64.
29. Landmann F, Orsi GA, Loppin B, Sullivan W. Wolbachia-mediated cytoplasmic incompatibility is associated with impaired histone deposition in the male pronucleus. *PLoS pathogens.* 2009; 5:e1000343. [PubMed: 19300496]

30. Werren JH. Biology of Wolbachia. *Annu Rev Entomol.* 1997; 42:587–609. [PubMed: 15012323]
31. Beckmann JF, Fallon AM. Decapitation Improves Detection of Wolbachia pipientis (Rickettsiales: Anaplasmataceae) in Culex pipiens (Diptera: Culicidae) Mosquitoes by the Polymerase Chain Reaction. *J Med Entomol.* 2012; 49:1103–1108. [PubMed: 23025192]
32. Chiu J, March PE, Lee R, Tillett D. Site-directed, Ligase-Independent Mutagenesis (SLIM): a single-tube methodology approaching 100% efficiency in 4 h. *Nucleic acids research.* 2004; 32:e174. [PubMed: 15585660]
33. Shrestha RK, et al. Insights into the mechanism of deubiquitination by JAMM deubiquitinases from cocrystal structures of the enzyme with the substrate and product. *Biochemistry.* 2014; 53:3199–3217. [PubMed: 24787148]
34. Sheedlo MJ, et al. Structural basis of substrate recognition by a bacterial deubiquitinase important for dynamics of phagosome ubiquitination. *Proceedings of the National Academy of Sciences of the United States of America.* 2015; 112:15090–15095. [PubMed: 26598703]
35. Mruk DD, Cheng CY. Enhanced chemiluminescence (ECL) for routine immunoblotting: An inexpensive alternative to commercially available kits. *Spermatogenesis.* 2011; 1:121–122. [PubMed: 22319660]
36. Schneider CA, Rasband WS, Eliceiri KW. NIH Image to ImageJ: 25 years of image analysis. *Nat Methods.* 2012; 9:671–675. [PubMed: 22930834]
37. Guthrie, CaFG. Guide to yeast genetics and molecular biology. *Methods Enzymol.* 1991; 194:1–863. [PubMed: 2005781]
38. Takeo S, et al. Shaggy/glycogen synthase kinase 3beta and phosphorylation of Sarah/regulator of calcineurin are essential for completion of Drosophila female meiosis. *Proceedings of the National Academy of Sciences of the United States of America.* 2012; 109:6382–6389. [PubMed: 22421435]
39. Sullivan, W., Ashburner, M., Hawley, RS. *Drosophila Protocols.* Cold Spring Harbor Laboratory Press; 2000.
40. Ritorto MS, et al. Screening of DUB activity and specificity by MALDI-TOF mass spectrometry. *Nat Commun.* 2014; 5:4763. [PubMed: 25159004]

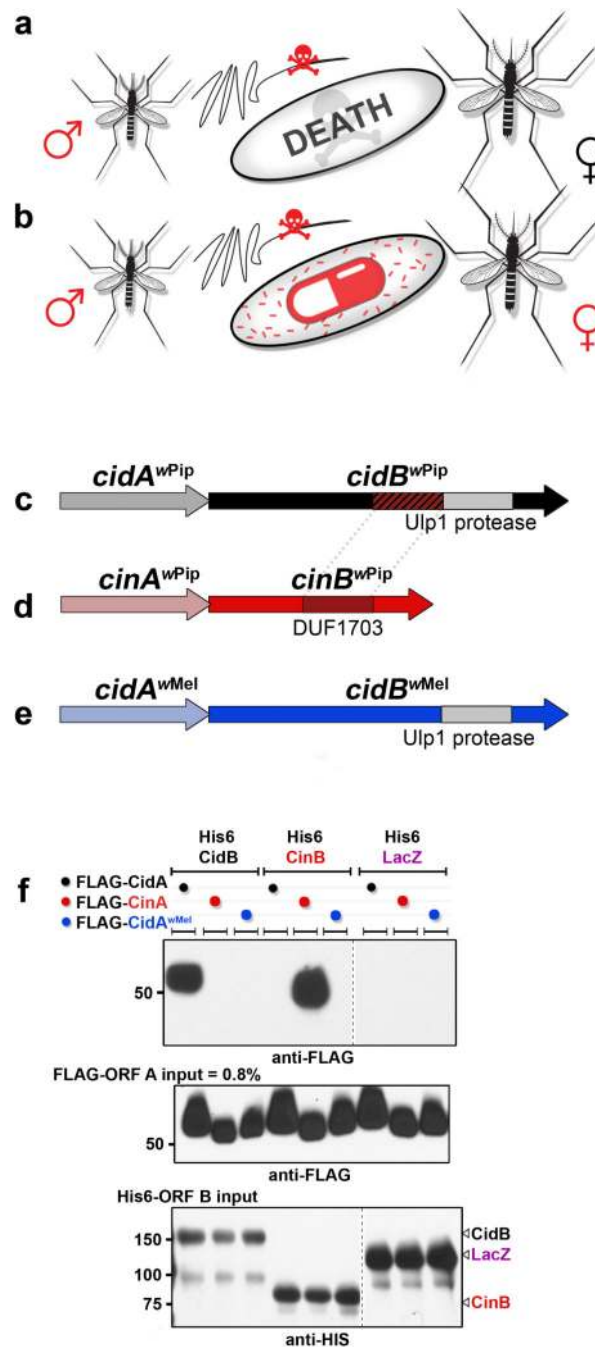


**Figure 1.**

Modification-Rescue hypothesis for CI. **a.** Crossing *Wolbachia*-infected males (red) with uninfected females (black) yields nonviable embryos due to a sperm-derived modification. **b.** Crossing infected males and similarly infected females rescues viability due to a rescue factor in the infected egg. **c.** Operon from *Wolbachia* (*wPip* strain) proposed to induce CI; the *wPa\_0282* and *wPa\_0283* genes encode CidA and the deubiquitylating enzyme CidB, respectively. **d.** Paralogous operon from *wPip* in which a putative DUF1703 nuclease, CinB (*wPa\_0295*) might also induce CI. **e.** Orthologous *cidA-cidB* operon from *wMel*, a

*Wolbachia* strain isolated from *D. melanogaster*. **f.** Pull-down assays of operon partners reveal interaction specificity (6 replicates). His6-tagged  $\beta$ -galactosidase (LacZ) is a negative control.

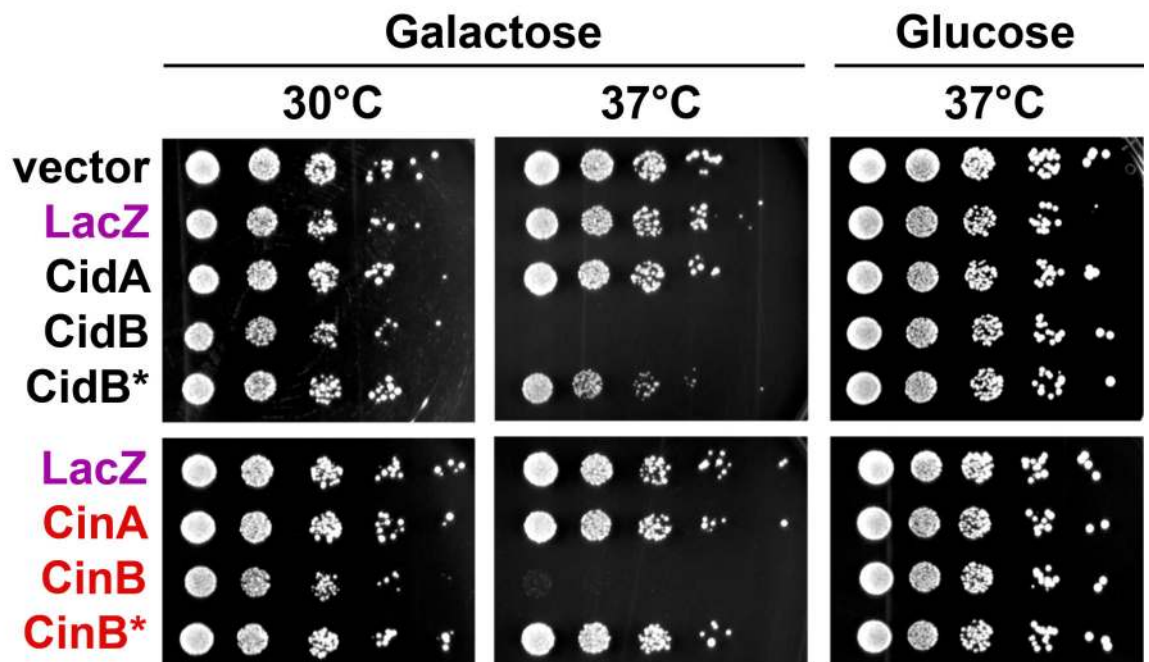
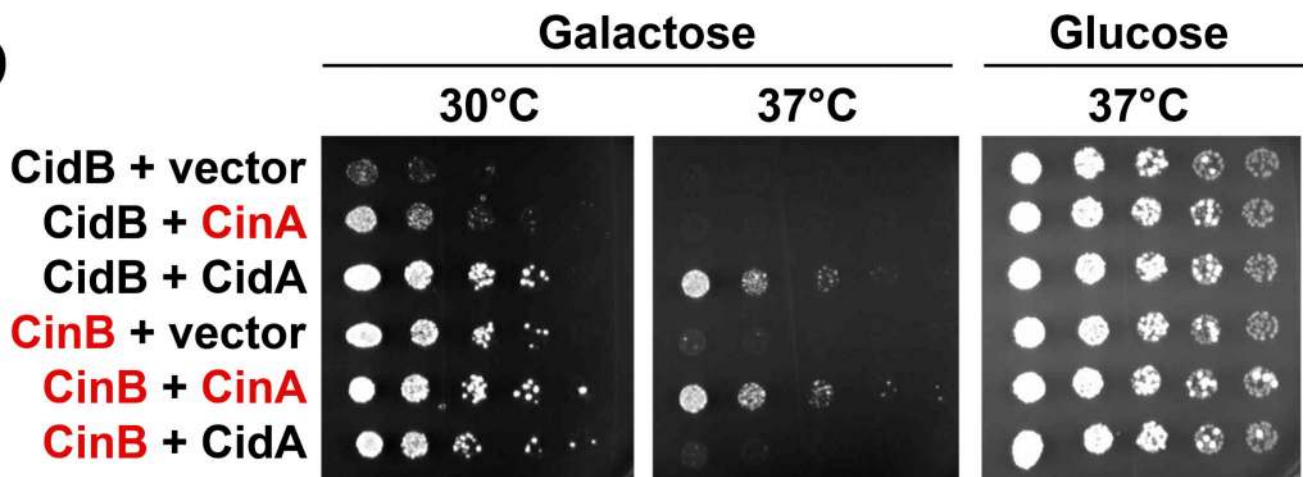
Author Manuscript

Author Manuscript

Author Manuscript

Author Manuscript



**a****b****Figure 2.**

Testing of the Modification-Rescue hypothesis in *Saccharomyces cerevisiae*. **a.** Expression of *Wolbachia* proteins from a galactose-inducible *GAL1* promoter on minimal medium lacking uracil and containing galactose or glucose (3 replicates). Control plasmids pYES2 (empty vector) and LacZ (negative control) cause no defects. Both CidB and CinB expression blocks yeast growth at high temperature. Inactivation of the Ulp1-like protease by a C1025A mutation (CidB\*) or the putative DUF1703 nuclease by mutation of the D-E-K triad to A-A-A (CinB\*) eliminates toxicity. **b.** Coexpression of CidB or CinB with different upstream operon components on minimal media lacking uracil and leucine shows growth rescue only with cognate partners (3 replicates). Vector is pRS425.

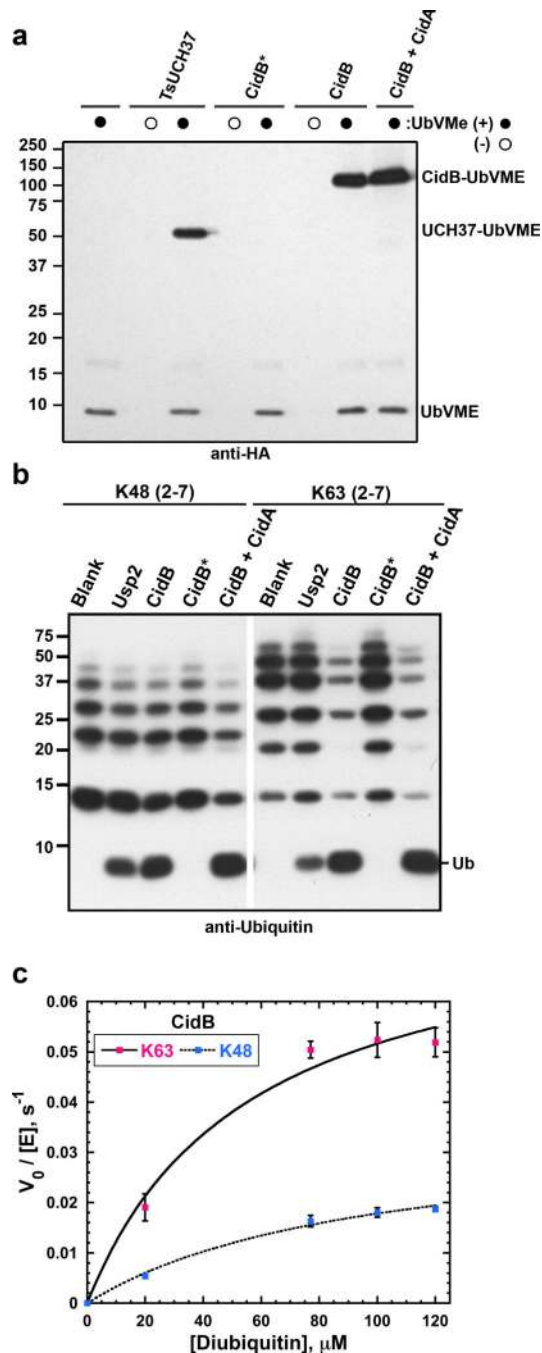


**Figure 3.** CidB is a DUB. **a.** DUB reactivity with the N-terminally HA-tagged suicide inhibitor, UbVME (3 replicates). Shown is an anti-HA immunoblot analysis of 30-min reactions performed at room temperature. UbVME reacts with the wild-type CidB protein but not the C1025A catalytic mutant (CidB\*). TsUCH37 is a positive control.<sup>23</sup> CidA at 100-fold molar excess does not inhibit UbVME reactivity. **b.** Cleavage by CidB of K48- and K63-linked ubiquitin chains assayed by anti-ubiquitin immunoblotting (3 replicates). Usp2 is a positive control.<sup>40</sup> Enzyme and polyubiquitin chains were at 50 nM and 500 nM, respectively, and

reactions were at 37°C for 1 h. **c.** CidB has a ~4-fold preference for K63-ubiquitin dimers compared to K48-linked dimers. Shown is a plot of initial velocity (divided by total enzyme concentration) as a function of substrate concentration from three independent experiments. Error bars are standard deviations.

Author Manuscript

Author Manuscript

Author Manuscript

Author Manuscript

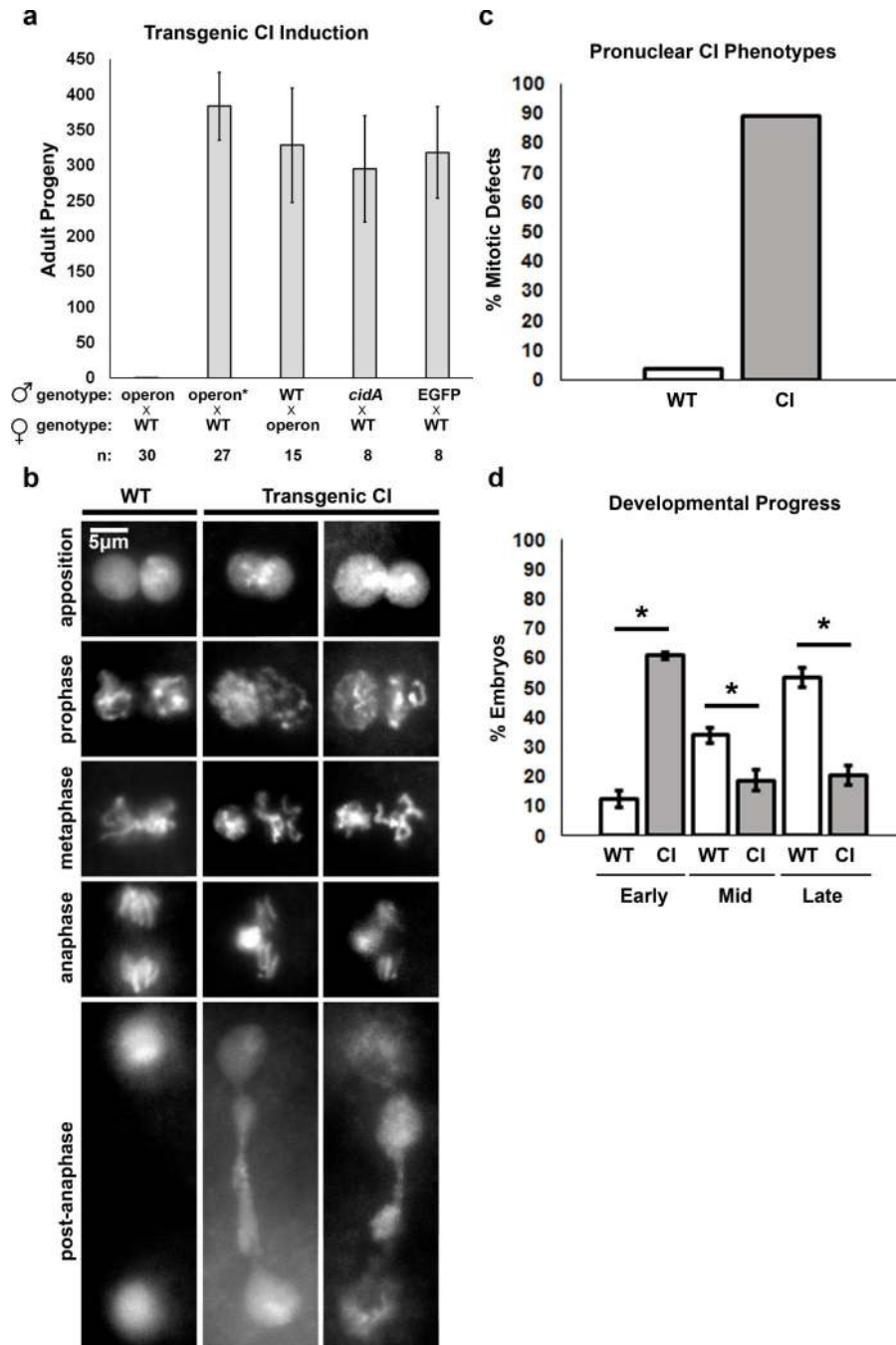


**Figure 4.** Induction of CI by transgenic *cidA-cidB* males. **a.** *D. melanogaster* males carrying transgenic *cidA-cidB* are sterile when mated to wild-type (WT) females (n=30 mating vials). Males with transgenic *cidA-cidB\** harboring the CidB active-site mutation C1025A (operon\*) are fully fertile as are females with the active transgenic operon. CidA by itself has no effect on fertility; no strain singly transgenic for *cidB* could be isolated. EGFP is a negative control. Error bars are standard deviations. **b.** CI-like defects in the male pronucleus initially appear in late prophase, during the first division of the apposed female and male

pronuclei, and accrue through mitosis. Abnormal cytology was observed in 56 transgenic CI embryos fixed after 18 min of development. **c.** Quantification of transgenic *cidA-cidB* (CI) embryos' mitotic defects including uncondensed paternal chromosomes, delayed segregation of paternal chromosomes, or chromosomal bridging during the first zygotic cell cycle. Sample sizes of observed transgenic and WT embryos were 63 and 29, respectively. **d.** Quantification of developmental progress in transgenic ("CI") embryos. At 24 h after egg laying, embryos were classified into three categories. Early, pre-blastoderm formation; Mid, blastoderm until segmentation stages; and Late, segmented stages. Quantification is based on three samples of approximately 200 embryos each. 60% of CI embryos arrested development in the early stage compared to 12% from the wild-type (WT) control. Significant *p* values (< 0.005) are indicated by (\*). Error bars are standard deviations.

Author Manuscript

Author Manuscript

Author Manuscript

Author Manuscript